Behavior of light at photonic crystal interfaces

Emanuel Istrate, Alexander A. Green, and Edward H. Sargent

Department of Electrical and Computer Engineering, University of Toronto, 10 King's College Road, Toronto, Ontario M5S 3G4, Canada

Band structures and Bloch modes give a generalized description of light in infinite photonic crystals. We show that the band structure and Bloch modes also contain the information necessary to find the amplitude and phase of light reflected and transmitted from interfaces in systems made using finite and semi-infinite photonic crystals. We obtain the equivalent of the Fresnel coefficients for photonic crystals. We use these coefficients to derive the reflection of light from a photonic crystal of finite size and the resonant modes of photonic crystal cavities and line defects. Results are given for ideal two-dimensional crystals, as well as crystals etched in semiconductor slab waveguides.

I. INTRODUCTION

Today there are two main ways of understanding the behavior of light in photonic crystals. Band structure[1] describes the allowed frequency bands in infinite photonic crystals. The corresponding Bloch modes describe electromagnetic field profiles in the crystals. Complex band structure[2,3] provides decay constants for evanescent waves inside the stop bands, in addition to the propagating wave vectors. On its own, however, band structure does not predict the behavior of crystals of finite size, especially near interfaces.

On the other hand, finite difference time domain (FDTD) simulations[4] are used to compute numerically the behavior of light in finite crystals. These simulations make no assumptions about the crystal periodicity, which makes them applicable to a wide range of structures; but, on their own do not offer generalizable insights. As a result, numerical simulations are mainly used for the design of finite photonic crystal structures on a case-by-case basis. Transmission and reflection at photonic crystal interfaces can also be computed in a variety of ways using transfer[5] or scattering matrices.[3] These methods take into account the periodicity of the crystal, but they are either unstable, when used with three-dimensional structures, or are designed for very specific crystals. Defects in photonic crystals have been computed using Wannier functions,[6] while sections of photonic crystal waveguide circuits and bends have been modeled using scattering matrices.[7] The response of slab waveguides with an infinite periodic pattern to light coming from the top has been modeled using scattering matrices[8] and Green function techniques.[9]

Notomi has derived a method to describe the refraction of light entering a photonic crystal[10] using equi-frequency surfaces computed from the band diagram and enforcing conservation of the lateral wavevector. However, the amplitude and phase of the waves reflected and transmitted at the interface are not determined.

Here we show that the photonic crystal bandstructure and Bloch modes contain all of the information necessary to compute the amplitude and phase of transmitted and reflected waves at interfaces between photonic crystals and homogeneous materials. While Notomi's work has applied Snell's law to photonic crystals, we derive herein the equivalent of complex-valued Fresnel coefficients in periodic structures. We use the complex band structure and Bloch modes, giving us results that are valid both inside and outside the stop bands. The complex band structure, together with Notomi's extension of Snell's law and the new Fresnel coefficients, allow us to develop a rigorous treatment of light in finite photonic crystals using a picture of propagation through locally homogeneous effective media.

It is possible to consider finite-sized crystals using an envelope approximation:[11,12] in such treatments, the fields at each frequency are described as superpositions of Bloch modes computed at other frequencies. In particular, evanescent modes are expressed mathematically in terms of superpositions of propagating modes. While this is justified by the fact that a complete basis set is used, a large number of modes is needed in the expansion for photonic band gap materials in which light is strongly forbidden.

In fact, the behavior of photonic crystal-based devices is conceptualized in terms of the propagation of light in certain regions of the device, and the decay of the fields in other regions. Herein we take the approach of expressing fields in terms of Bloch modes—propagating or decaying, depending on whether light is allowed or forbidden—as they are excited by incident fields.

The transmittance and reflectance of light from a finite photonic crystal has been modeled before using a plane-wave expansion and boundary effects[13] and a similar problem has been solved using Green functions[14] for two-dimensional crystals. However, both methods consider the entire crystal at once and the computation becomes more difficult as the size of the structure increases. The periodicity of the crystal is not used to provide the salient properties of band structure, such as propagation or decay. In contrast, we use the periodicity of the crystal to obtain solutions valid for any size and geometry of photonic crystal and we calculate the boundary conditions explicitly.

We start by computing the complex band structure of photonic crystals, in order to produce results both inside and outside photonic crystal stopbands. We then derive the boundary conditions at the interface and use them to calculate the reflectance at photonic crystal interfaces. As ex-

amples, we use these results to compute the transmittance and reflectance from finite-size crystals, where multiple reflections can occur between the two interfaces, and the resonant states of two-dimensional cavities. We finish by computing the resonant state in a line defect fabricated in a semiconductor slab waveguide.

II. THE COMPLEX BAND STRUCTURE

To quantify reflection and transmission at the interface, we require the band structure and Bloch modes for a given frequency and wave vector parallel to the interface. We employ an extension of the plane-wave expansion method (PWEM).[15] The PWEM solves for the allowed frequencies as eigenvalues of

$$\sum_{\mathbf{G}'} |\mathbf{k}+\mathbf{G}'|^2 \eta_{\mathbf{G}-\mathbf{G}'} \begin{pmatrix} \hat{e}_{\mathbf{G}}^2 \cdot \hat{e}_{\mathbf{G}'}^2 & -\hat{e}_{\mathbf{G}}^2 \cdot \hat{e}_{\mathbf{G}'}^1 \\ -\hat{e}_{\mathbf{G}}^1 \cdot \hat{e}_{\mathbf{G}'}^2 & \hat{e}_{\mathbf{G}}^1 \cdot \hat{e}_{\mathbf{G}'}^1 \end{pmatrix} \begin{pmatrix} A_{\mathbf{G}'}^1 \\ A_{\mathbf{G}'}^2 \end{pmatrix}$$
$$= \frac{\omega^2}{c^2} \begin{pmatrix} A_{\mathbf{G}}^1 \\ A_{\mathbf{G}}^2 \end{pmatrix}, \qquad (1)$$

with the magnetic field modes given by

$$\mathbf{H} = \sum_{\mathbf{G}} \sum_{\lambda=1,2} |\mathbf{k}+\mathbf{G}| A_{\mathbf{G}}^\lambda \hat{e}_{\mathbf{G}}^\lambda e^{i(\mathbf{k}+\mathbf{G}) \cdot \mathbf{r}}, \qquad (2)$$

where $\mathbf{G}$ and $\mathbf{G}'$ are reciprocal lattice vectors. $\eta_{\mathbf{G}-\mathbf{G}'}$ contains the Fourier components of the dielectric structure and $\hat{e}_{\mathbf{G}}^\lambda$ describes the polarizations of the plane waves. In the usual application of the method, one chooses a vector $\mathbf{k}$ and computes the corresponding frequency eigenvalues of the matrix on the left-hand side.

A method has previously been proposed[2] to compute the complex band structure by replacing $\mathbf{k}$ with complex values. This, however, gives rise to an extensive search, since for many choices of $\mathbf{k}$ there will only be complex frequency eigenvalues.

Our approach is similar to that introduced for complex Bloch modes in semiconductors.[16] Complex Bloch modes are of importance only near crystal edges, i.e., before they decay to zero. For this reason, only the component of the Bloch wave vector perpendicular to the edge should be complex. We therefore manipulate Eq. (1) to treat this component as the eigenvalue. We decompose the Bloch wave vector into components parallel and perpendicular to the interface, $\mathbf{k} = \mathbf{k}_\parallel + \hat{z} k_z$, assuming that the interface is perpendicular to the $\hat{z}$ direction. As with interfaces between homogeneous materials, $\mathbf{k}_\parallel$ has to be conserved across the interface, while k_z does not.[10] We thus assume that $\mathbf{k}_\parallel$ and ω are known.

We separate Eq. (1) in the different orders of k_z and write the result as a matrix equation:

$$k_z^2 \mathbf{M}_a A + k_z \mathbf{M}_b A + \mathbf{M}_c A = 0, \qquad (3)$$

where $\mathbf{M}_a$, $\mathbf{M}_b$, and $\mathbf{M}_c$ are independent of k_z. These are square matrices of size N containing the coefficients from Eq. (1). $\mathbf{M}_c$ contains the frequency ω. A is a column vector containing the elements $A_{\mathbf{G}}^\lambda$. Equation (3) can be written as an eigenvalue equation for k_z using a square matrix of size $2N$,
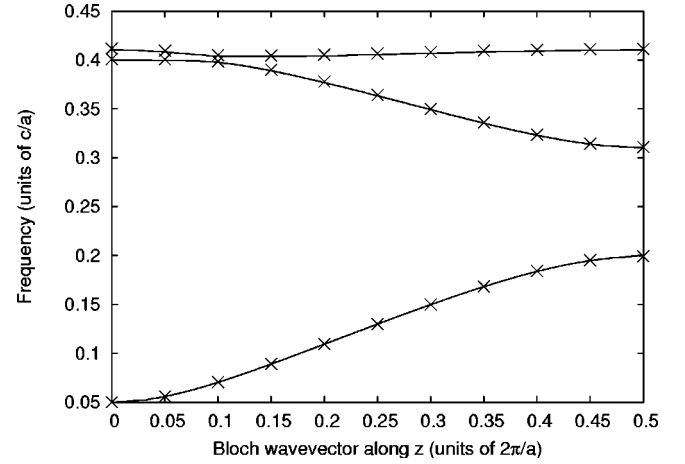

FIG. 1. Real bands for a square lattice of silicon cylinders in air. $n=3.4$, $r=0.3a$, $k_x=0.2\pi/a$. The lines represent our data. The points are calculated using MPB.

$$\begin{bmatrix} 0 & \mathbf{I} \\ -\mathbf{M}_a^{-1}\mathbf{M}_c & -\mathbf{M}_a^{-1}\mathbf{M}_b \end{bmatrix} \begin{pmatrix} A \\ k_z A \end{pmatrix} = k_z \begin{pmatrix} A \\ k_z A \end{pmatrix}. \qquad (4)$$

The above matrix is non-Hermitian; its eigenvalues are in general complex. Real eigenvalues appear for propagating modes in the allowed frequency regions. Modes with small imaginary parts of k_z decay slowly and are the most important in slices of photonic crystals.

As an example, Fig. 1 shows the real part of the band structure as a plot of frequency versus k_z for a square two-dimensional crystal of silicon cylinders in air. The cylinders have a radius of $0.3a$ with their axes oriented in the $\hat{y}$ direction. We consider the TM polarization, where the electric field is parallel to the cylinders and find the modes with a constant k_x of $0.2\pi/a$. 4096 plane waves are used in the expansion. The plot compares the results with the original PWEM used by the MIT Photonic Bands package, MPB.[17]

Figure 2 shows the lowest imaginary band of the same structure. This describes the attenuation of a wave propagating in the stop band of the crystal. The computation was
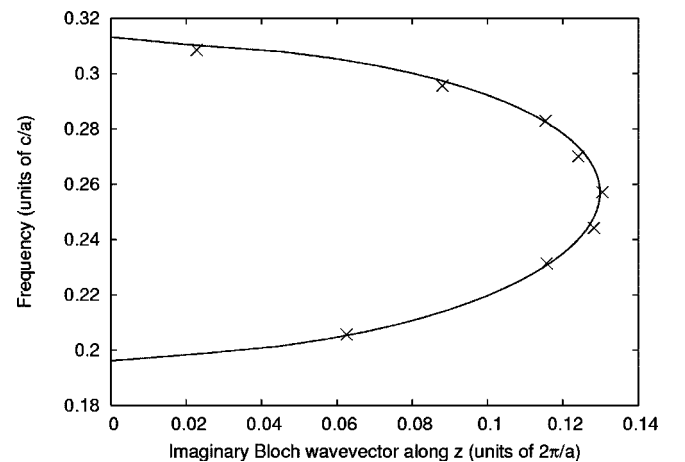

FIG. 2. Imaginary bands for a square lattice of silicon cylinders in air. $r=0.3a$, $k_x=0$. The line represents our data. The points are calculated using FDTD.
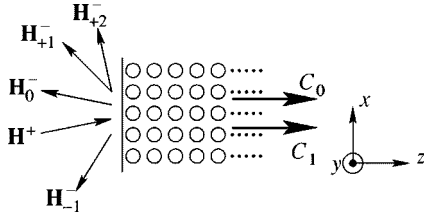
FIG. 3. Waves considered at the boundary. $\mathbf{H}^+$ and $\mathbf{H}_0^-$ are the incident and reflected waves in the homogeneous material. $\mathbf{H}_{\pm1}^-$, $\mathbf{H}_{\pm2}^-,\ldots$ are the waves diffracted by the crystal. They may be propagating or evanescent. C_j are the photonic crystal Bloch modes excited at the interface.

done using $k_x=0$. For comparison, the attenuation of the crystals has been computed using FDTD, by simulating the transmittance through crystals of various lengths and fitting the results to an exponential decay. A fine grid of 32×32 points per unit cell was used in the FDTD calculations to minimize numerical dispersion.

III. PHOTONIC CRYSTAL BOUNDARY CONDITIONS

We now know the modes in which light is allowed to exist in a photonic crystal, both in the stop band and outside. We also know the modes of the structures surrounding the crystal, usually plane waves. To find the reflection and transmission coefficients at a photonic crystal interface is to compute the amplitude and phase of the modes excited by an incoming wave. The incoming wave is a mode of either the photonic crystal or the surroundings and will excite modes in both regions. We present a mode-matching technique to find the excited modes.

At the interface the usual electromagnetic boundary conditions of continuity of the tangential components of the electric and magnetic fields must hold. This means that the superposition of modes on the two sides of the interface must have the same profile and periodicity. The periodicity of the mode in the crystal is determined by the lattice. We decompose the modes in the plane of the interface into two-dimensional spatial Fourier series. The modes must be matched for each spatial Fourier frequency independently.

To illustrate the concept, we assume an interface between a homogeneous material on the left and a two- or three-dimensional photonic crystal on the right. The interface is perpendicular to the z direction, at $z=0$. Light is incident from the left, as a plane wave with magnetic field $\mathbf{H}=\mathbf{H}^+e^{i\mathbf{k}_0\cdot\mathbf{r}}$. The input light will excite a set of real or complex Bloch modes in the crystal, and a set of diffracted waves, propagating or evanescent, in the homogeneous material, as illustrated in Fig. 3.

On the left of the interface, the superposition is

$$\mathbf{H}_h = \mathbf{H}^+ e^{i\mathbf{k}_{0,\parallel}\cdot\mathbf{r}} e^{ik_{0,z}z} + \sum_m \mathbf{H}_m^- e^{i\mathbf{k}_{m,\parallel}\cdot\mathbf{r}} e^{-ik_{m,z}z}. \tag{5}$$

$\mathbf{H}^+$ and $\mathbf{H}_m^-$ contain the amplitude and phase of the incident and diffracted waves. $\mathbf{k}_{m,\parallel}$ is the wave vector component parallel to the interface of the mth diffracted wave. All the plane waves must have lateral propagation vectors equal to Fourier

components of the photonic crystal modes, $\mathbf{k}_{m,\parallel}=\mathbf{k}_{0,\parallel}+\mathbf{G}_{m,\parallel}$. $\mathbf{k}_{0,\parallel}$ for the incident wave may lie in the first Brillouin zone of the crystal or outside, depending on the angle of the incident wave. $k_{m,z}=\sqrt{(\omega n/c)^2-k_{m,\parallel}^2}$ may be imaginary. In that case the diffracted waves have a significant amplitude only near the photonic crystal surface. The boundary conditions for the magnetic field become

$$\mathbf{H}_{m,\parallel}^+ + \mathbf{H}_{m,\parallel}^- = \sum_j C_j \mathbf{H}_{j,m}^C, \tag{6}$$

where we have used $\mathbf{H}_m^+=\mathbf{H}^+$ for $m=0$ and $\mathbf{H}_m^+=0$ otherwise. j labels the photonic crystal modes and C_j gives their complex amplitude. $\mathbf{H}_{j,m}^C$ represents the tangential magnetic field of the mth Fourier component of photonic crystal mode j in the plane of the interface. It can be obtained from the complex PWEM described above or by other methods. Using Eq. (2) we can write

$$\mathbf{H}_{j,m}^C = \left(\sum_{\mathbf{G}|\mathbf{G}_{m,\parallel}} \sum_\lambda |\mathbf{k}+\mathbf{G}| A_{\mathbf{G}}^\lambda \hat{e}_{\mathbf{G}}^\lambda \right)_{\parallel}. \tag{7}$$

The first sum above is done over all $\mathbf{G}$ vectors with a fixed $\mathbf{G}_{m,\parallel}$.

Enforcing the boundary conditions for electric field yields a similar set of equations:

$$\mathbf{E}_{m,\parallel}^+ + \mathbf{E}_{m,\parallel}^- = \sum_j C_j \mathbf{E}_{j,m}^C, \tag{8}$$

where $\mathbf{E}_{m,\parallel}^\pm$ are the electric field components of the plane waves in the homogeneous material. $\mathbf{E}_{j,m}^C$ is the tangential electric field of the mth Fourier component of photonic crystal mode j in the plane of the interface. It can again be written in terms of the plane wave expansion

$$\mathbf{E}_{j,m}^C = \frac{1}{\omega\epsilon_c} \left(\sum_{\mathbf{G}|\mathbf{G}_{m,\parallel}} \sum_\lambda |\mathbf{k}+\mathbf{G}|(\mathbf{k}+\mathbf{G}) \times \hat{e}_{\mathbf{G}}^\lambda A_{\mathbf{G}}^\lambda \right), \tag{9}$$

where ϵ_c is the dielectric constant of the photonic crystal background material.

Equations (6) and (8) can be solved to find the unknown complex amplitudes of the modes excited in the crystal, C_j, as well as the waves diffracted back to the left, $\mathbf{H}_m^-$. A similar set of equations is obtained for light incident from the photonic crystal onto the interface.

At frequencies with a single allowed Bloch mode, which appear frequently in the first stop band of a crystal and below it, the equations can be simplified further. We consider only the Fourier component with the smallest spatial frequency, $m=0$, and define $n_C=|\mathbf{H}_{0,0}^C|/|\mathbf{E}_{0,0}^C|\sqrt{\mu_0/\epsilon_0}$. Writing $k_{0,z}=n_h\cos(\theta_h)\omega/c$, where n_h and θ_h represent the index of refraction of the homogeneous medium and the direction of the incident wave, we obtain for a TM incident wave

$$r_{\text{TM}} = \frac{H_0^-}{H^+} = \frac{n_C\cos(\theta_h)-n_h}{n_C\cos(\theta_h)+n_h}, \tag{10}$$
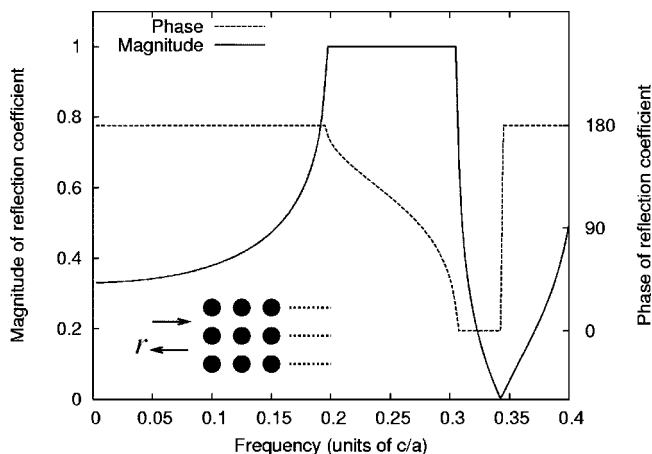
and for a TE incident wave

FIG. 4. Magnitude and phase of the reflection coefficient from a semi-infinite photonic crystal. The insert shows the geometry considered.

$$r_{TE} = \frac{n_C - n_h \cos(\theta_h)}{n_C + n_h \cos(\theta_h)}. \qquad (11)$$

These are the reflection coefficients of light from a photonic crystal. They resemble the Fresnel equations for homogeneous media. n_C represents an effective refractive index of the crystal. Inside the stop band n_C becomes imaginary, producing a reflection coefficient of unit magnitude.

In Fig. 4 we plot the phase and magnitude of the reflection coefficient r for light reflected from a semi-infinite 2D photonic crystal. We use the same crystal as in Fig. 1. We consider the TM polarization, i.e., the electric field vector is parallel to the cylinders. The direction of the input beam is perpendicular to the photonic crystal surface. The insert shows a diagram of the structure. In the later examples we also apply the boundary conditions for light incident at an angle, and for the three-dimensional problem of a crystal etched in a thin semiconductor slab.

In our calculations we keep within the extended Brillouin zone representation of the band diagram and remain on the same branch of the dispersion relation when traversing a stop band.

The phase response in reflection. As shown in Fig. 4, the reflection phase from photonic crystals changes from 0 to 180° when going from one stop band edge to the other one. This can be explained in terms of the photonic crystal modes at the two stop band edges. With the directions shown in Fig. 3, we assume that the incoming plane wave has the electric field polarized along the y direction and the magnetic field along x.

It is known that at the lower stop band edge of a crystal, the electric field is predominantly concentrated in the high-index region of each unit cell, while at the upper stop band edge the opposite is true.[18] The magnetic field acts in the opposite manner from the electric field. In the case presented here, the interface between the crystal and air is in a low-index area of the photonic crystal unit cell. Hence, at the lower stop band edge we expect a strong magnetic field at the interface, while at the upper edge we expect a strong
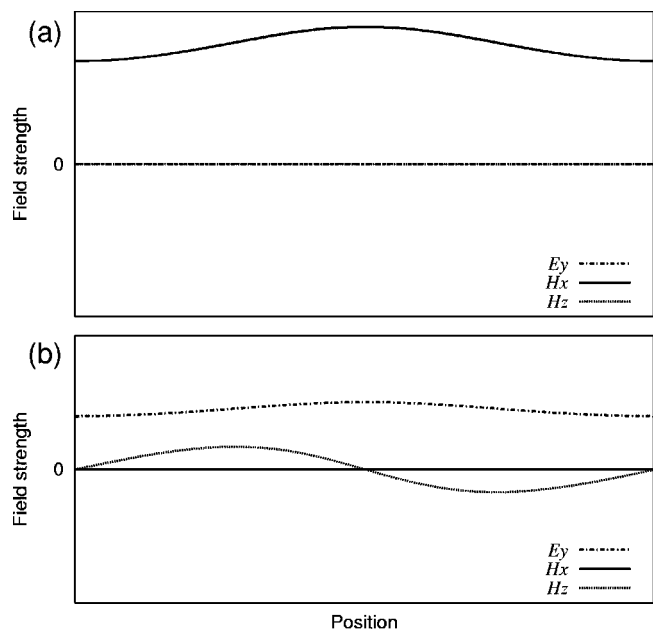

FIG. 5. Electric and magnetic fields of the photonic crystal Bloch modes at the edge of the unit cells, at the lower (a) and upper (b) edge of the first stop band.

electric field. Figure 5 shows the electric and magnetic fields of the band-edge Bloch modes at the edges of the unit cells. We use the same crystal and polarization as the one from Fig. 4.

At the lower band edge the only nonzero field component in the crystal is H_x. Matching a superposition of an incoming and a reflected plane wave to these fields, requires that the E_y components of the two plane waves cancel. As a result, reflection at this point is similar to that from a perfect electric conductor. At the upper band edge the situation is reversed. H_x is zero, which forces the magnetic field components of the incoming and reflected waves to cancel. Reflection is like that from a perfect magnetic conductor. At this band edge, however, the crystal also has a nonzero H_z. Although this component is not tangential to the interface and does not appear in our boundary conditions, it must have a corresponding field component on the other side of the interface. This field component does not appear in the incoming or reflected wave and must be matched to higher-order diffracted waves of the crystal, denoted by $\mathbf{H}_{\pm 1}^- \mathbf{H}_{\pm 2}^-, \dots$ in Fig. 3. In the case presented here, and in almost all cases of practical interest for normal incidence, the diffracted waves are evanescent, which means that they do not carry power, and only influence the field distribution near the interface. Higher-order diffraction is also required in order to satisfy the non-uniform values of H_x and E_z at the two band edges.

The phase response depends on the distribution of electric and magnetic fields in the crystal. For an inverted crystal, such as a crystal made by etching holes in a semiconductor, the lower band edge will have the electric field near the interface. The phase response in this crystal would be the opposite. The reflection would be like that from a magnetic conductor at the lower band edge, and like an electric conductor at the upper edge.
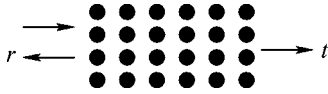
FIG. 6. Finite-size photonic crystal used to compute reflectance and transmittance.

IV. TRANSMITTANCE THROUGH FINITE PHOTONIC CRYSTALS

Knowledge of the transmission and reflection at the interfaces, combined with the propagation and decay inside the crystal, allow us to understand photonic crystals of finite size. All measurements of reflection or transmission of light from photonic crystals are made using finite crystals in which multiple reflections between the interfaces lead to fringes in the spectrum outside the stop bands, similar to Fabry–Perot fringes between two mirrors. The fringes have been seen experimentally[19] ever since thin high-quality photonic crystal films have been fabricated. The example structure considered here is shown in Fig. 6.

We compute the reflection spectrum of such a finite photonic crystal using Airy's formulas[20] to sum the multiple reflections at the two interfaces

$$r = r_{12} + \frac{t_{12}t_{21}r_{23}e^{2i\phi}}{1 - r_{21}r_{23}e^{2i\phi}}, \qquad (12)$$

where ϕ is the product of the Bloch wave vector and the thickness of the crystal. r_{ij} and t_{ij} represent the reflection and transmission coefficients from layer i into j obtained earlier. The results are shown in Fig. 7. Figure 7(a) contains the magnitude of the reflection from the semi-infinite photonic
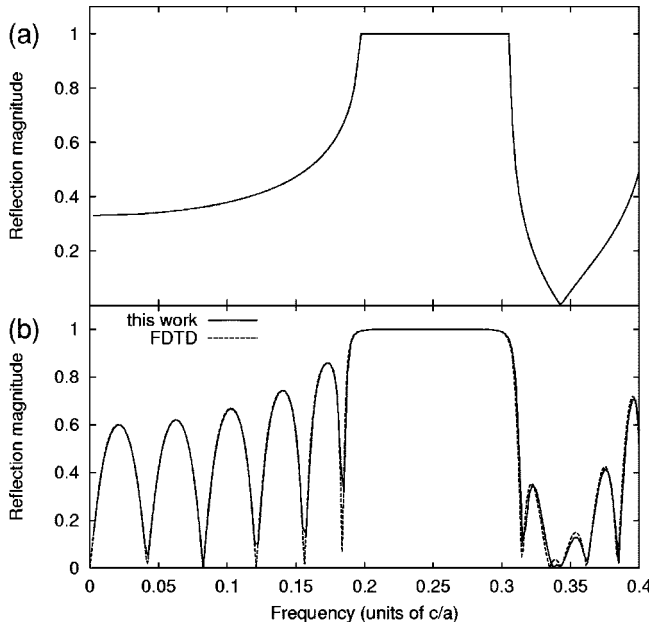

FIG. 7. (a) Magnitude of reflection coefficient from the semi-infinite photonic crystal. (b) Magnitude of reflection from a finite photonic crystal consisting of six periods, solid line is obtained from the reflection and transmission of semi-infinite crystals, dashed line is from FDTD.
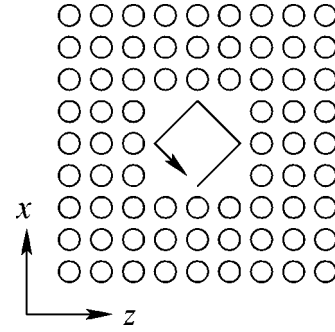

FIG. 8. Schematic diagram of the resonant cavity considered.

crystal, obtained earlier. In Fig. 7(b) we plot (solid lines) the magnitude of the reflection from the crystal; results of the corresponding FDTD simulations are given by dashed lines. Our model agrees with full simulations very well in magnitude and position of the fringes.

Using the complex bandstructure and Bloch modes in finite structures assumes that the modes of the infinite crystals are excited. This approximation is usually good; however, in photonic crystals with very few layers it loses its validity. If the crystal from Fig. 7(b) is reduced to only two layers, there will be an error of up to 8% in the reflection spectrum, since the two layers do not have sufficient periods to manifest the modes predicted within a band structure picture.

V. MODES OF TWO-DIMENSIONAL CAVITIES

Photonic crystals inhibit propagation of light in more than one direction, enabling formation of high quality factor cavities in two-dimensional crystals.[6] Such cavities have been shown to be useful as high-finesse drop filters.[21,22] Using knowledge of the reflection phases at the interfaces, we describe the resonant states of the cavities such as the one shown in Fig. 8.

The treatment is analogous with that of quantum-mechanical states in quantum wires. Propagating waves in the cavity are connected to decaying fields in the crystal using the boundary conditions. The waves in the cavities must interfere constructively with themselves upon successive round-trips, in order to produce a resonant state. This resonance condition must be enforced in both directions in the cavity. We use L_x and L_z for the dimensions of the cavity and k_x and k_z for the propagation constants in the two directions. The effect of the photonic crystal is included through the phase of the reflection coefficients, $\phi_x(k_z, \omega)$ and $\phi_z(k_x, \omega)$, computed earlier. $\phi_x(k_z, \omega)$ is the phase change upon reflection from an interface parallel to the z direction. It depends on frequency and also on the incident angle of the incoming wave. This incident angle is determined by k_z. In the same manner, ϕ_z describes reflections at interfaces parallel to the x direction and depends on k_x and ω. With these definitions, the resonance conditions are

$$k_x L_x + \phi_x(k_z, \omega) = l\pi, \quad k_z L_z + \phi_z(k_x, \omega) = m\pi, \qquad (13)$$

where l and m are two integers.

In Fig. 9 we show the modes for square cavities with sizes between one and five lattice constants, obtained by removing
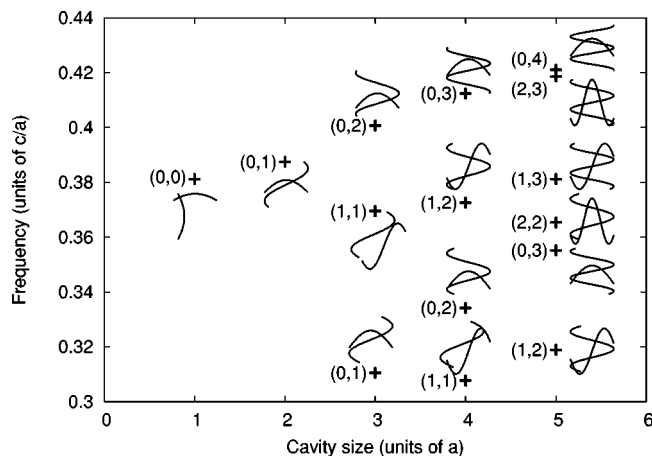
FIG. 9. Resonant modes of square cavities vs cavity size. Crystal has a square lattice of Si cylinders in air, $r=0.2a$. Points mark the resonant frequencies; numbers represent the mode numbers by counting the nulls in the mode in the x and z direction; curves represent the part of the mode profile that lies inside the cavity, in the two directions.

several cylinders from a square two-dimensional crystal of Si cylinders in air. The cylinder radius is 0.2 times the lattice constant and we consider again the TM polarization. When comparing the resonant frequencies with full numerical simulations, we obtain an agreement of 0.6% in frequency.

Once the resonant frequencies are found using Eq. (13), the mode profiles are readily obtained. Inside the cavity, the modes are given by the superposition of plane waves, with propagation constants $\pm k_x$ and $\pm k_z$. Outside the cavity they are given by the decaying Bloch modes computed by our plane-wave expansion. The decay depends on frequency and on the incident angle of the wave from the cavity onto the crystal. It is given by the complex band structure. This can be used to determine the effective mode volume in the cavity.

VI. MODELING THREE-DIMENSIONAL STRUCTURES

The above-presented examples have used two-dimensional structures in order to simplify the illustrations and to allow rigorous comparisons with full simulations. The complex band structure and boundary conditions can also be calculated for devices with variations in three dimensions. Both two-dimensional photonic crystals etched in a semiconductor slab waveguide, as well as crystals periodic in all three dimensions can be considered.

In this section we model the resonant states of a line defect formed in a photonic crystal of air holes etched in a thin silicon membrane with air on both sides. The crystal is a square lattice of air-holes etched in the membrane. A diagram of the structure is shown in Fig. 10. We assume that light will resonate in this structure in a direction perpendicular to the defect. The lattice constant is a. The slab thickness is $h =0.5a$ and the hole radius is $0.3a$. We find width of the line defect W, required for a certain resonant frequency.

The decaying stop band modes of the photonic crystal are found using a three-dimensional plane-wave expansion,
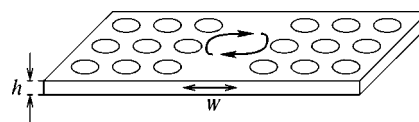

FIG. 10. Slab waveguide resonant structure, consisting of a silicon membrane with holes etched through it.

similar to the description in Sec. II. The line defect is interpreted as a thin unpatterned slab waveguide between two photonic crystals. The reflection coefficients at the interface between the waveguide and the crystal are computed in a manner similar to the one described in the previous sections. However, instead of matching the photonic crystal modes to plane waves, we matched them to modes of the unpatterned slab. The defect width versus resonant frequency are shown in Fig. 11. We use modes with even symmetry in the plane of the membrane, similar to TE modes of the corresponding two-dimensional crystal.[23] We compare our results with MPB simulations at the points where the defect width is equal to a multiple of a. We obtain an agreement in the position of the resonant states with respect to the stop band edges of better than 2% of the stop band width. The structure can also be employed as a photonic crystal waveguide. The guided modes and dispersion relation can be found by repeating the above simulations using a propagation vector along the guide.

VII. CONCLUSIONS

We have shown that the complex amplitude of transmitted and reflected waves at photonic crystal boundaries can be obtained from the complex Bloch modes and band structure of the crystals. These results, combined with those of Ref. 10, provide complete information about the behavior of light at photonic crystal interfaces. Together with the propagation and decay constants from the complex band structure they allow us to interpret photonic crystals as effective media whose key properties are given by their respective band
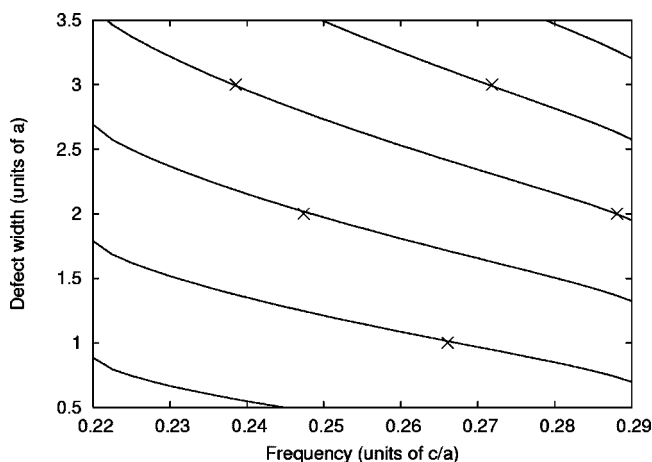

FIG. 11. Defect width required for a given resonance frequency for a line defect in a photonic crystal etched in a silicon membrane. Lines are our model, points are from MPB simulations.

structures. Structures with variations in both two and three dimensions can be considered. Since the reflection, transmission, and diffraction coefficients depend only on the photonic crystal structure and surrounding medium, these can be computed in advance for subsequent use. Many different devices can then be simulated and optimized very quickly using these data. This technique can be directly applied to the computation of modes in photonic crystal waveguides[24] and resonant cavities, coupling of light from waveguides to photonic crystals, as well as light traversing any number of photonic crystals.

In combination with a multiple-scales method,[25,26] this approach could also be used to compute the response of finite photonic crystals including nonlinearities. The boundary conditions would determine how light enters the crystal, while propagation inside the crystal would be handled by the multiple-scales equations. A similar method could be used for the reflection and transmission coefficients from crystals with fabrication imperfections, using the eigenmodes of the perfect crystal, while considering the deviations from this in a perturbative approach.

[1] K. M. Leung and Y. F. Liu, Phys. Rev. Lett. **65**, 2646 (1990).

[2] T. Suzuki and K. L. Yu, J. Opt. Soc. Am. B **12**, 804 (1995).

[3] N. Stefanou, V. Karathanos, and A. Modinos, J. Phys.: Condens. Matter **4**, 7389 (1992).

[4] K. S. Yee, IEEE Trans. Antennas Propag. **14**, 302 (1966).

[5] P. M. Bell, J. B. Pendry, L. M. Moreno, and A. J. Ward, Comput. Phys. Commun. **85**, 306 (1995).

[6] K. Busch, S. F. Mingaleev, A. Garcia-Martin, M. Schillinger, and D. Hermann, J. Phys.: Condens. Matter **15**, R1233 (2003).

[7] S. F. Mingaleev and K. Busch, Opt. Lett. **28**, 619 (2003).

[8] D. M. Whittaker and I. S. Culshaw, Phys. Rev. B **60**, 2610 (1999).

[9] A. R. Cowan, P. Paddon, V. Pacradouni, and J. F. Young, J. Opt. Soc. Am. A **18**, 1160 (2001).

[10] M. Notomi, Phys. Rev. B **62**, 10696 (2000).

[11] C. M. de Sterke and J. E. Sipe, Phys. Rev. A **38**, 5149 (1988).

[12] E. Istrate, M. Charbonneau-Lefort, and E. H. Sargent, Phys. Rev. B **66**, 075121 (2002).

[13] K. Sakoda, *Optical Properties of Photonic Crystals* (Springer, New York, 2001), Chap. 4.

[14] M. Paulus and O. J. F. Martin, Phys. Rev. E **63**, 066615 (2001).

[15] K. Busch and S. John, Phys. Rev. E **58**, 3896 (1998).

[16] D. L. Smith and C. Mailhiot, Phys. Rev. B **33**, 8345 (1986).

[17] S. G. Johnson and J. D. Joannopoulos, Opt. Express **8**, 173 (2001).

[18] J. D. Joannopoulos, R. D. Meade, and J. N. Winn, *Photonic Crystals: Molding the Flow of Light* (Princeton University Press, Princeton, 1995).

[19] J. F. Bertone, P. Jiang, K. S. Hwang, D. M. Mittleman, and V. L. Colvin, Phys. Rev. Lett. **83**, 300 (1999).

[20] P. Yeh, *Optical Waves in Periodic Media* (Wiley, New York, 1988).

[21] Y. Akahane, M. Mochizuki, T. Asano, Y. Tanaka, and S. Noda, Appl. Phys. Lett. **82**, 1341 (2003).

[22] B. S. Song, S. Noda, and T. Asano, Science **300**, 1537 (2003).

[23] S. G. Johnson, S. Fan, P. R. Villeneuve, J. D. Joannopoulos, and L. A. Kolodziejski, Phys. Rev. B **60**, 5751 (1999).

[24] E. Istrate and E. H. Sargent, IEEE J. Quantum Electron. **41**, 461 (2005).

[25] N. A. R. Bhat and J. E. Sipe, Phys. Rev. E **64**, 056604 (2001).

[26] J. L. Sheriff, I. A. Goldthorpe, and E. H. Sargent, Phys. Rev. E **70**, 036616 (2004).